Available online at www.sciencedirect.com

ScienceDirect

Energy Procedia 81 (2015) 995 – 1004

Energy Procedia

69th Conference of the Italian Thermal Engineering Association, ATI 2014

Application of a novel method for a simulation of conductivity of a building material in a climatic chamber

Giorgio Pia[a], M. Ludovica Casnedi[a], Roberto Ricciu[b]*, Luigi Antonio Besalduch[b], Roberto Baccoli[b], Costantino Carlo Mastino[b], Roberto Innamorati[b], Arianna Murru[a], Ombretta Cocco[a], Paola Meloni[a],Ulrico Sanna[a]

[a] *Dipartimento di IngegneriaMeccanica, Chimica e dei Materiali,Università degli Studi di Cagliari, Piazza d'Armi, Cagliari, 09123, Italy*
[b] *Dipartimento di Ingegneria Civile, Ambientale e Architettura, Università degli Studi di Cagliari, Piazza d'Armi, Cagliari, 09123, Italy*

Abstract

This work proposes the application of a new simulation method based on fractal geometry for the calculation of the thermal conductivity for building materials. The results obtained are compared with the measurement, in a climatic chamber, of the heat flow through a material chosen as the sample. The test sample is made with "pietracantone", a stone widely used as a building material and as an ornamental stone in the areas of Cagliari and Sassari in Sardinia. This material is characterized by a limestone matrix and a porosity which significantly influences the value of thermal conductivity. It is not known to the authors that this material had already been studied for its thermal properties.

Peer-review under responsibility of the Scientific Committee of ATI 2014

Keywords: Thermal conductivity, Thermal transmittance measurement, Fractal geometry, Pore size distribution

1. Introduction

Buildings energy consumption accounts for a 20–40% of total energy use in developed countries [1], so the correct evaluation of thermal conductivity is an important factor in defining the total energy consumption of heating and cooling systems and achieving optimal thermal comfort for occupants. In particular too little attention is paid to the

* Corresponding author. Tel.: +39-070-675-5379; fax: +39-070-675-5818.
E-mail address: ricciu@unica.it

Peer-review under responsibility of the Scientific Committee of ATI 2014
doi:10.1016/j.egypro.2015.12.158

energy consumption of monuments and historic district. For this reason the authors studied the thermal conductivity of stones that compose this ancient buildings. In Cagliari, stone has been used for the construction of historical monuments, from the 13th century, i.e. wall fortifications, pisan towers etc., to 19th century, i.e. municipal building, still inhabited although in the winter season occur thermo hygrometric discomfort. These buildings are often protected by the Superintendence of Cultural Heritage and it is not possible the adoption of typical modern solutions used for new buildings. For this reasons, it is very important to develop a new method to evaluate physical properties of building materials without damage historical sites. One of these is represented by fractal modelling. Fractals are figures characterized by self-similarity, non-integer dimension, irregularity, etc. They are able to reproduce nature shapes and also microstructures of several materials. So, in this paper we compared two test methods: a new computational fractal method [2-5] for the study of microstructures simulation and a simulation in a climatic chamber using a full-sized walls with realistic inner and outer wall climatic conditions. This procedure is carried out using "Pietracantone" (Canton stone). It is a sedimentary rock (limestone) of Miocene age from Sardinia west coast that in technical terms may be defined as calcareous stone, porous, easy workability, but poor durability if maintained in permanent contact with water. This lithotype is, in terms of porosity and mechanical properties, substantially equivalent to others that have been used, like this one, to build in the monuments of many areas of the Mediterranean.

Nomenclature

k_{eff}	thermal conductivity of sample	[W/mK]
k_{calc}	fractal model thermal conductivity	[W/mK]
k_f	thermal conductivity of fluid	[W/mK]
k_s	thermal conductivity of solid phase	[W/mK]
a	height of the specimen	(mm)
b	width of the specimen	(mm)
h	dept of the specimen	(mm)
i	iteration number to cover porosimetric range	
n	B units number (integer)	
D_f	fractal dimension of Sierpinski carpet	
R_{max}	maximum pore ray dimension	(μm)
R_{min}	minimum pore ray dimension	(μm)
ε	fractal model pore fraction	
ε_{exp}	experimental pore fraction	
C_s	Specific Conductance	[W/m^{2}K]

2. Test Methods

The use of fractal geometry was be used to derive analytical expression to obtain physical quantities and to simulate the porous microstructures, this approach is well known in literature [6- 9]. The fractal geometry is also able to describe the heat transference process, and analytical expression can give thermal conductivity value [10], because the heat flow is influenced by the low volume fraction of the solid phase, by the conductivity of the gas enclosed, by the size of the cell and pores, etc. [11]. In order to identify the thermal conductivity of the Pietracantone, the mineralogical phases which constitute this biomicritic limestone, X-ray powder diffraction analysis were carried out using a Rigaku Miniflex II diffractometer operating with a Cu-Kα monochromatic, wavelength at 15 kV. Mercury intrusion porosimetry is used to know porosity and pore size distribution (Auto Pore IV - Micrometrics). In particular an Intermingled Fractal Units (IFU) procedure was be used, in order to correlate the thermal conductivity of the specimen under test with the pore size distribution.
These values are later compared with those obtained with the experimental simulation in the climatic chamber.

2.1. Analytical Method: The Intermingled fractal units model

The intermingled fractal units model, in order to represent experimental pore size distributions in stone materials and advanced ones, has been used.

The proposed approach is essentially based on:

- reproduction of a experimental pore size distribution (fractal or non-fractal), with fractal units; these units are the Sierpinski carpet obtained by repeatedly removing squares from an initial square of unit side-length. The non-iterated sub-squares are named “solid forever”. The Fig. 1 shows three iterations (1,2 and 3) of the Sierpinski carpet [9]. IFU model consists of two types basic units proposed in different configurations and sizes(1 unit A and n units B). While the number of iteration increases, the geometrical structure is fine, highly intricate and detailed at all scales (Fig.1). The number of units B is: $n = (A_{Ap}-\varepsilon \cdot AA) / (\varepsilon \cdot A_B-A_{Bp})$ with A_A, A_B, A_{Ap} e A_{Bp} , respectively the total area and the area of the pores belonging to units A and B which make up the IFU (Fig. 2);
- To ensure that the porosity is constant by varying the pore size distribution, it was necessary to introduce sufficient parts of IFU filled surface. As happens to “solid forever” the "filled surface" is a non porous portion of the model.
- definition of the fractal pattern of the porous microstructures using continuous units and definition of the circuit diagram of the units, in which, by using series and parallel combinations, we obtain k_{eff} (assuming in this case that at each subsequent iteration of the scaling k_{eff} is the calculation result of the previous stage, Fig. 3);
- estimating macrostructure thermal conductivity value through a new circuit diagram which allows to evaluate possible different solid or fluid phases which will give rise to combinations of the microstructure and thus different values of k_{eff} (depending of the articulation of the circuit diagram) which will be processed through a calculation of the average.

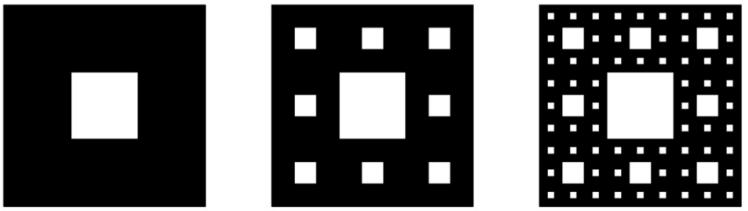

Fig. 1. Sierpinski carpet (Three iterations).

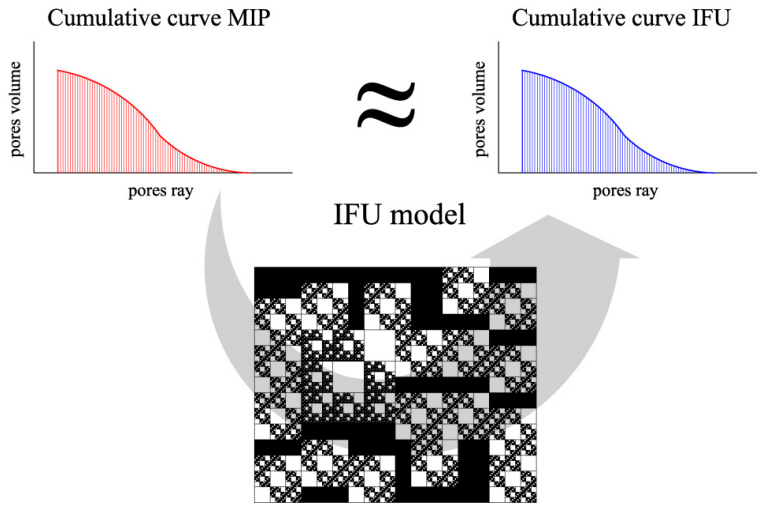

Fig. 2. IFU elaboration.

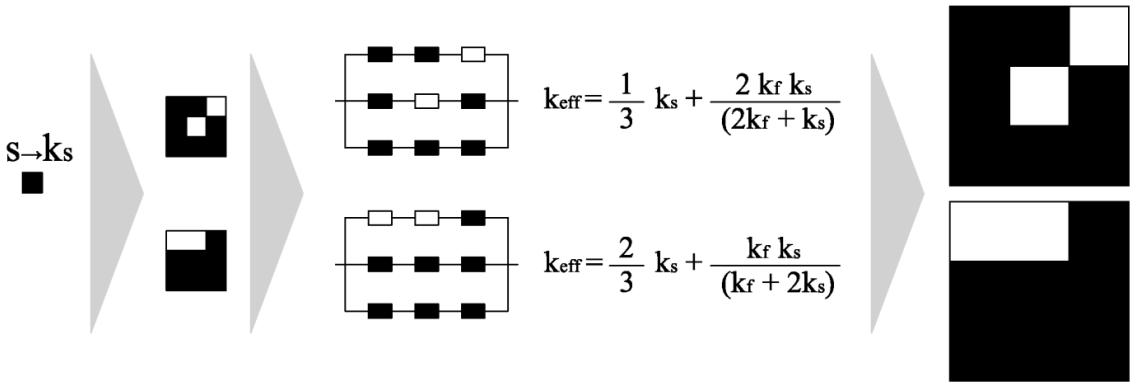

Fig. 3.IFU procedure to calculate thermal conductivity step by step.

For example for the case in which two pores are in different line k_{eff} value is:

$$k_{eff} = \frac{2 \cdot k_f \cdot k_s}{2k_f + k_s} + \frac{1}{3} k_s \qquad \text{[W/mK]} \qquad (1)$$

While for the pattern in which pores are in the same line k_{eff} value is:

$$k_{eff} = \frac{k_f \cdot k_s}{k_f + 2k_s} + \frac{2}{3} k_s \qquad \text{[W/mK]} \qquad (2)$$

This first cell is part of the next stage of fractal modelling, whenever it is taken as part of "solid", with a k_s equivalent to the value of k_{eff} that has been calculated before. Therefore, as a general remark, we can say that, the value of k_{eff} calculated at the n-th iteration stage is inserted into step (n + 1)th as the new value of the conductivity of the "solid" phase, by using the same expression.
A number of possible and different configurations of connections in series and parallel for the same system will be then processed in order to get an average thus eventually obtaining a k_{calc} that can be compared with the data acquired experimentally.

2.2. Experimental Method and Measurements

The measures obtained with the previous model were compared with those obtained with a climatic simulation chamber (Fig. 4) that allows testing of full-sized walls with realistic inner and outer wall climatic conditions [12] and it was designed according to the UNI EN ISO 1934:2000, ISO 9869:1994 and EN 12494:1996.The apparatus consists of two chambers and a frame through which it is possible to measure and control: air temperature, relative humidity and air velocity.
The geometric size of the test stone was measured with a vernier caliber and the dimension is shown in Table 1; a, b and h are defined in the Fig. 5a and it was inserted into a frame (Fig. 5b - 5c) of polyurethane foam having density of 40 kg/m^3 and thermal Conductivity showed in the Fig. 6.

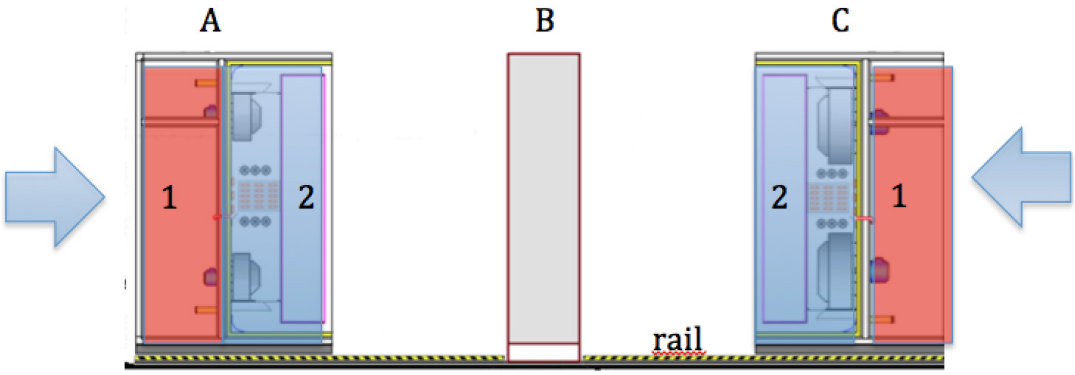

Fig. 4. Climatic chamber, vertical section. (A) Indoor chamber, (C) Outdoor Chamber. The specimen is contained in a frame(B) between the two chamber.1 is the compartment electrical control system, 2 is the compartment air handling. The arrows indicate that the chamber A and C move on rails (dashed line and the yellow at the base of the chamber) to close in the frame B.

Table 1. Geometrical test size.

a (mm)	b (mm)	h (mm)
500 ± 0.5	500 ± 0.5	110 ± 0.25

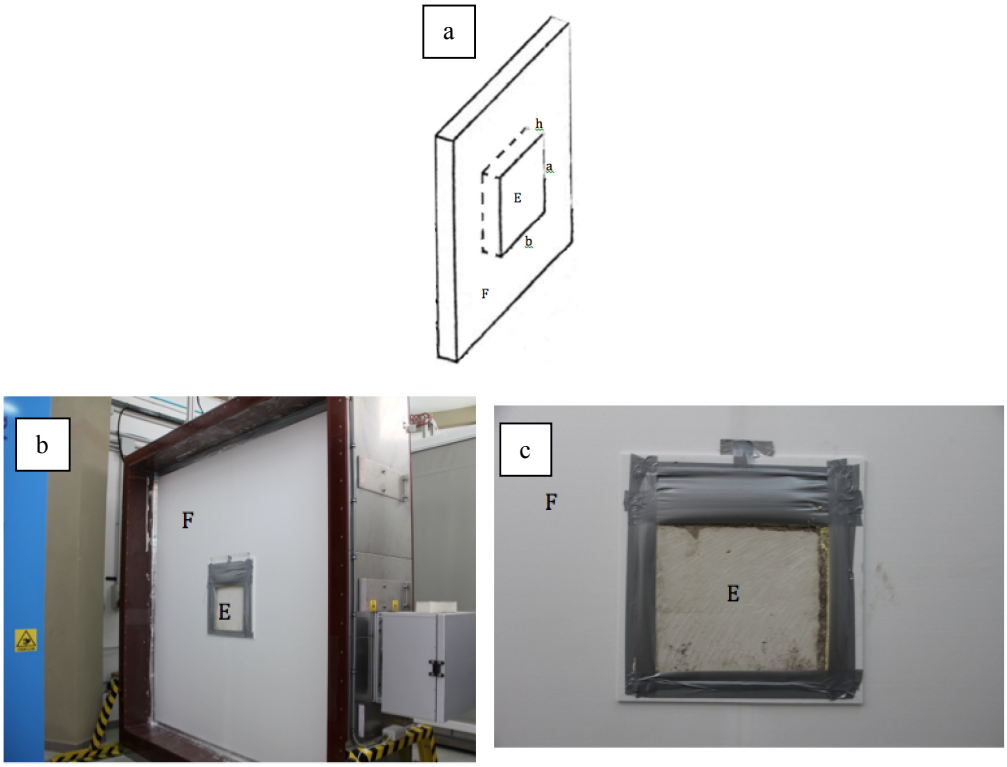

Fig. 5. The test stone (E) is contained in a frame of polyurethane . (a) Geometrical representation of the specimen, (b) Picture of the frame containing the specimen, (c) Detail of the specimen

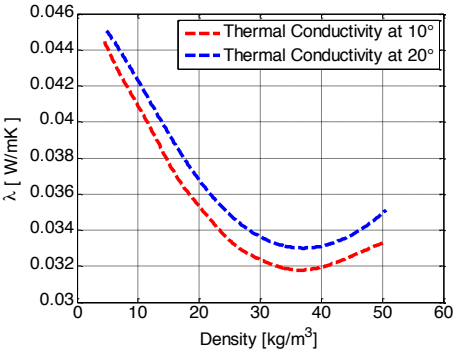

Fig. 6.Value of the Thermal Conductivity of the Polyurethane in relation of the volumic mass (Density). The red dashed line represents the thermal conductivity at 10°C, the bluedashed line at 20°C.

The test stone was instrumented by means of RTD (resistive temperature detector) sensors for the surface temperature measurement. The indoor air temperature was measured by means of NTC (negative temperature coefficient) thermistors. Heat-flux sensors were fixed to the wall to measure the surface temperature and heat-flux.
In order to obtain sufficient data, six RTD sensors and two heat-flux sensors (which also include two temperature thermopile sensors) were fixed. On the wall cold face, two RTD sensors and two heat-flux meters were set up to avoid thermal radiation on them. A sample rate measurement of 5min was chosen, taking into account the variation velocity of the environmental parameters measured. Surface temperatures and heat-flux output data were returned by a wireless data logger, while air temperatures in the two chambers by TGU2 data loggers. The data were subsequently transferred and processed through dedicated spreadsheets.
The method requires, the measurement of surface temperatures and heat-flux through the test stone by the use of heat-flux meters [13 - 14]. All sensors and measurements systems are provided with individual calibration certificates by Italian Calibration Service SIT. The instruments used were heat flux and superficial temperature sensors.
The heat flux meter consists of:

- Four sensors of RTD 1000 thermal measurement in Class 1/3 B by standard DIN/IEC75. The external superficial finishing of the sensors is similar to the plaster in order to have a similar absorption coefficient of solar radiation. The wiring to the radio modem consists of wave electrical wire to minimize the electromagnetic interference.
- The heat flux sensor is the FE01-3B model. The primary sensing element is a cylindrical thermopile sensor. The contact surface has an 80 mm radius and the thickness is 5,5 mm. The main metro logical characteristics are: span (measurement field): −300 to 300 W/m2 ; resolution 0,01 W/m2 ; unbias: ±5%.

The measuring chain is also composed of wireless wiring in the ISM 2,4 GHz band and is compatible with the IEEE 802.15.4 protocol. The system also includes a data logger with integrated RAM.
The main metrological characteristic software and data logger are: resolution 16 bit, 30 channels and maximumsampling speed is 1 min on each of the 30 channels.
In this instrumentation class extreme synchronism in acquisition times is not necessary and therefore the data come from the single channel through multiplexer technologies. In this application the data logger is programmed for maximum performance and the internal software calculates the mean value every five consecutive data and stores this value in its RAM. surface temperature sensors are applied on the wall in several different ways so as to guarantee an elastic constant force. The methods are mainly mechanical and chemical.

3. Results

3.1. Analytical results

Following the steps above illustrated, it is possible to obtain a simulation of the experimental porosimetric

curves. Table 2 shows the input data to set up the IFUmodel, it shows the porosimetric intervals, the number of units used and their fractal dimensions.
In Fig.7is shown a comparison between experimental and model pore cumulative curve, for four different specimen of the same kind of stone: A, B, C and D (tab. 2). It is clear that IFU model is able to reproduce real microstructure even if they are not fractal.

Table 2. IFU input data to model A, B,C ad D.

		A	B	C	D
1 Unit A	D_f	1,89	1,89	1,89	1,89
	R_{max} (μm)	44	44,81	44,73	44,77
	Iteration	7	7	7	7
	R_{min} (μm)	0,02	0,02	0,02	0,02
	solid forever	5	6	5	5
n Unit B	D_f	1,77	1,77	1,77	1,77
	n	$2{,}31\cdot10^3$	$2{,}55\cdot10^3$	$2{,}79\cdot10^3$	$2{,}79\cdot10^3$
	R_{max} (μm)	1,63	1,66	1,66	1,66
	iteration	4	4	4	4
	R_{min} (μm)	0,02	0,02	0,02	0,02
	solid forever	2	2	2	2
	filled surface (μm^2)	$3{,}32\cdot10^4$	$7{,}08\cdot10^4$	$8{,}32\cdot10^4$	$4{,}84\cdot10^4$
	ε_{exp} tot / ε_{calc} tot (%)	35,9/35,9	32,85/32,85	33,09/33,09	36/36

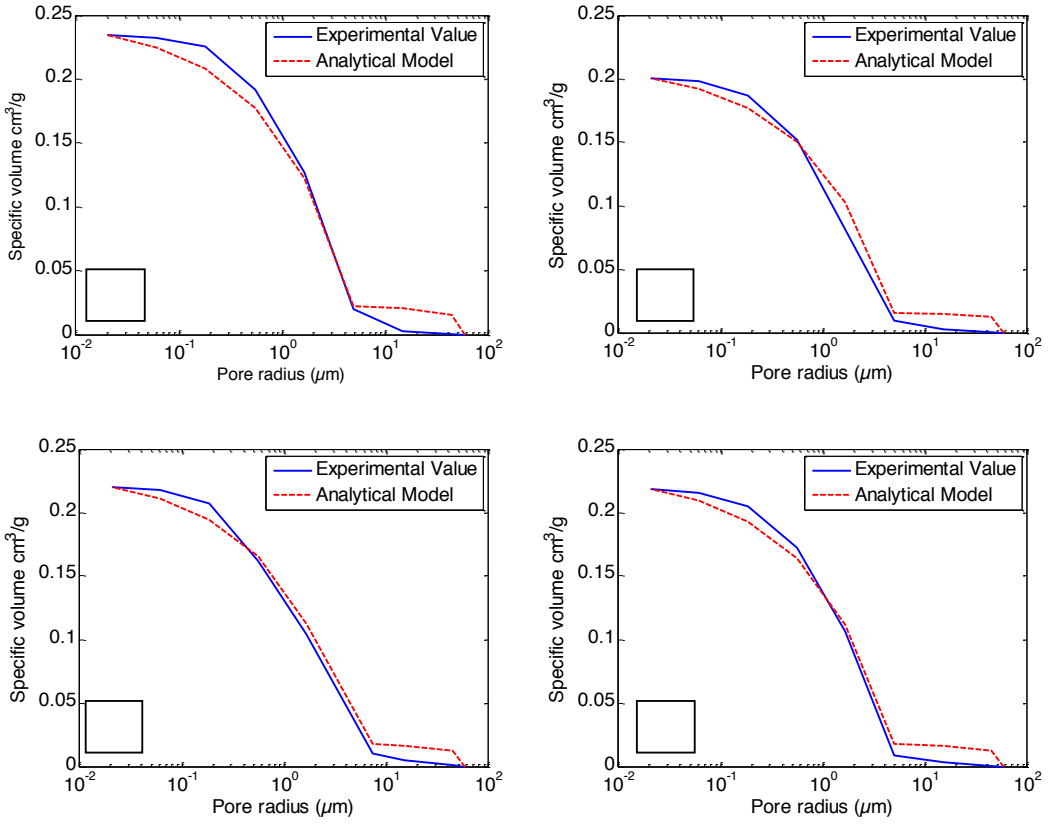

Fig. 7.Porosimetric cumulative curve: experimental (blue line) and model (red dashed line)

By converting these configurations in electrical patterns it is possible to calculate thermal conductivity step by step.
The interpretation of the diffractogram through JCPDS [15] database highlighted the presence of calcite as predominant phase. Other carbonate minerals were represented by ankerite and dolomite while detritical phases were proved by the presence of quartz and muscovite. For this reason k_s = 3,5W/(m·K), while k_f = 0,026 W/(m·K) are considered. So, the k_{eff} average value calculated by IFU procedure is 1,27 W/(m·K) while experimental value (considering that the thickness of the sample is 0,11 m) is 1,21 ± 0,12 W/(m·K). It is possible to see that calculated and experimental data are compatible. Indeed, the success of this procedure is certainly attributable to its relevance with the experimental data and with the actual microstructure of the material.

3.2. Experimental results: Measurement and results

In the Climatic Chamber, the test began with the following environmental conditions held constant in the two chambers for 12 hours: Air temperature: about 50°C; Relative humidity: about 10%; Air Velocity: about 1 m/s.
Two series of measurements were carried out, both lasting longer than 72 h.
The two chambers have been programmed to simulate the stationary conditions summarized in the table 3.

Table 3. Simulation condition.

	Indoor Chamber	Outdoor Chamber
Air temperature [°C]	8	33
Relative humidity [%]	20	20
Air velocity [m/s]	0,1	1,0

The measurements were carried out maintaining a mean surface temperature difference between the indoor and the outdoor chamber of about 10°C, see Fig. 8.

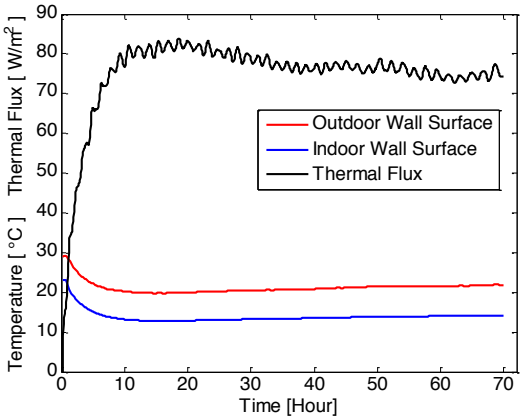

Fig. 8.Surface wall temperature in the indoor (blue line) and outdoor (red line) chamber, and Thermal Flux (black line)

It is possible to notice that the temperature difference (ΔT) is more of 10 °C, becomes stable after a period of settling due to the delay of the temperature setting system. This justifies an increasing variation of the heat flux as reported in an example in Fig. 8.
The heat flux settles as the surface wall temperature difference becomes constant (after about12hours).
A measurement analysis was carried out with the progressive mean method according to the EN 12494:1996 standard (Fig. 9).
The results of the specific conductance C_s analysis are as shown in the Fig. 9: 11,05 ± 5%[W/m^{2}K]

and, if the nominal value of "h" in table 1 is 0,11 [m], the fictitious conductivity is equal to 1,10 ± 0,05 [W/mK].

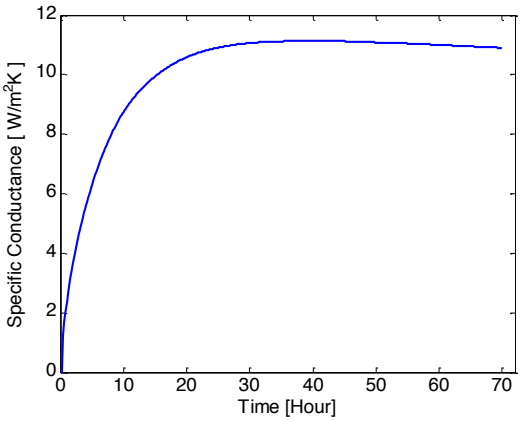

Fig. 9. Specific conductance

4. Conclusions

According to our preliminary results, the fractal model can approximate the experimental values obtained in the climatic chamber. The difference between the two values is possibly due to the dependence of the heat flow on the volume fraction of the solid phase, on the conductivity of the gas enclosed, and on the size of the cell and pores. So a greater number of specimen and of experimental simulations are needed to minimize the dependence of the results on the different unpredictable initial and boundary conditions.
The difference between the two representation is approximately the 9%, important in these values is that the two models, having an unbias of the 5%, have common coverage factor (there are common values between the unbias of the two methods).

Acknowledgements

"Gratefully acknowledges Sardinia Regional Government for the financial support (P.O.R. Sardegna F.S.E. Operational Programme of the Autonomous Region of Sardinia, European Social Fund 2007-2013 - Axis IV Human Resources, Objective l.3, Line of Activity l.3.1 "Avviso di chiamata per il finanziamento di Assegni di Ricerca").

References

[1] Asdrubali F., Bonaut M., Battisti M., Venegas M., Comparative study of energy regulations for buildings in Italy and Spain, Energy and Buildings 40 (2008) 1805–1825.
[2] Pia G., Sanna U., A geometrical fractal model for the porosity and thermal conductivity of insulating concrete, Construction and Building Materials 44 (2013) 551-556.
[3] Pia G., Sanna U., Intermingled fractal units model and electrical equivalence fractal approach for prediction of thermal conductivity of porous materials, Applied Thermal Engineering 61 (2013) 186-192.
[4] Pia G., Sanna U., Case studies on the influence of microstructure voids on thermal conductivity in fractal porous media, Case Studies in Thermal Engineering 2 (2014) 8-13.
[5] Pia G., Sanna U., An intermingled fractal units model to evaluate pore size distribution influence on thermal conductivity values in porous materials, Applied Thermal Engineering 65 (2014) 330-336.
[6] Tang H.P., Wang J.Z., Zhu J.L., Ao Q.B., Wang J.Y., Yang B.J., et al., Fractal dimension of pore-structure of porous metal materials made by stainless steel powder, Powder Technol. 217 (2012) 383-387.

[7] Zeng Q., Luo M., Pang X., Li L., Li K., Surface fractal dimension: an indicator to characterize the microstructure of cement-based porous materials, Appl. Surf. Sci. 282 (2013) 302-307.
[8] Zheng Q., Yu B., Duan Y., Fang Q., A fractal model for gas slippage factor in porous media in the slip flow regime, Chem. Eng. Sci. 87 (2013) 209-215.
[9] Pia G., Sanna U., An intermingled fractal units model and method to predict permeability in porous rock, Int. J. Eng. Sci. 75 (2014) 31-39.
[10] Huai X., Wang W., Li Z., Analysis of the effective thermal conductivity of fractal porous media, Appl. Therm. Eng. 27 (2007) 2815-2821.
[11] Lorna M.F.A., Gibson J., Cellular solids, Struct. Prop. 9 (1989) 165-166.
[12] Ferrari S., Zanotto V., The thermal performance of walls under actual service conditions: Evaluating the results of climatic chamber tests, Costruction and Building Materials 43 (2013) 309-316.
[13] Desogus G., Mura S., Ricciu R., Comparing different approach to in situ measurement of building components thermal resistance, Energy and Buildings, 43 (2011) 2613-2620
[14] UNI EN ISO 9869:1994, Thermal insulation - building elements - in situ measurement of thermal resistance and thermal transmittance.
[15] http://www.icdd.com